Strength and Rigidity Performance of Laminated Members Using Small-Diameter Logs

Been Ha   Sang Sik Jang   Keita Ogawa
Mariko Yamasaki   Yasutoshi Sasaki

Abstract

Korea and other countries have a high ratio of small-diameter logs in the harvested log volume. Hence, using these small-diameter logs as structural materials is an important issue. The lumber obtained from small-diameter logs generally has small cross-section dimensions and is mostly juvenile wood, resulting in inferior strength performance. In this research, a laminating process was developed for effective utilization of small-diameter logs as structural materials, and eight types of laminated beams and eight types of laminated columns were manufactured by the vertical and horizontal laminations with square cross-section timber. The laminated members were composed of laminated square timber obtained from small-diameter logs and were reinforced by square timber or lamina obtained from large-diameter logs. The laminated members were evaluated for their bending and axial compression performance. As a result, the beam exhibited an increase in bending Young's modulus of 63 percent and bending strength of 77 percent. Additionally, the column's axial compression performance indicated a positive effect on compression Young's modulus, where a 158 percent increase was found. Furthermore, when Johnson's equation was used to determine the critical stress, the value was close to the yield stress. In contrast, Euler's equation led to overestimation of the capacity as the slenderness ratio became smaller, which indicated that the application of Johnson's equation may be preferable. Therefore, a combination of small-diameter logs and large-diameter logs provided increased strength and rigidity performance, indicating the possibility of an effective use of small-diameter logs.

Korea relies on imported timber for the vast majority of their wood despite possessing significant timber resources. Recently, the development of forestry and forest product industry based on the utilization of domestic wood as well as the consideration of global environmental issues (e.g., low carbon emissions) has become quite important. Hence, the production of wood products from domestic forests is a desirable goal.

In Korea, efforts have been undertaken to improve the self-sufficiency for logs, reaching 58.5 percent in 2014 (Korea Forest Service 2015). Considering that the ratio was 28.1 percent in 2005, this is a sharp improvement. Meanwhile, self-sufficiency for lumber remains at 16.7 percent, indicating that the country still relies on imported timber.

Logs are classified by diameter as small, medium, and large (Korea Forest Service and Korea Forestry Promotion Institute 2013). Small-diameter logs have diameters at a breast height of 60 to 170 mm and a high ratio of juvenile wood, which leads to low strength accompanied by many knots, splits, and warps. Because the yield rate for lumber falls when juvenile wood is removed from small-diameter logs, their utilization as lumber and structural materials has not significantly advanced.

In Korea, the ratio of small-diameter logs to the total cutting volume is very high, with small-diameter logs accounting for 86.2 percent of the timber thinning, 65.1 percent of the regeneration cutting, and 79.8 percent of the other categories, as shown in Figure 1 (Korea Forest Service
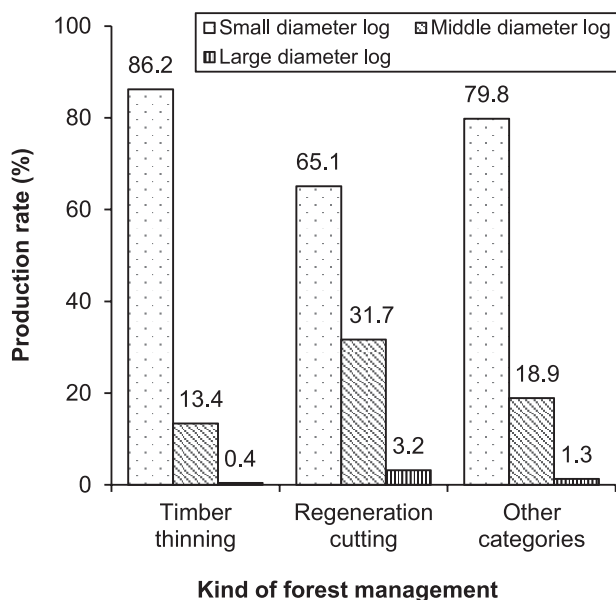
Figure 1.—Production rate of diameter class by forest management in Korea.

and Korea Forestry Promotion Institute 2013). Therefore, small-diameter logs account for the vast majority of Korea's forest cutting volumes. Because most small-diameter logs include juvenile wood, their utilization is limited to boards, chips, energy, and other low-value-added products. As a result, at the present time, many of the small-diameter logs cut are not harvested. Other countries also cut small-diameter logs for thinning for fire prevention and ecosystem diversity. However, these countries and Korea are not using their small-diameter logs efficiently. Using these types of small-diameter logs as raw materials for high-value-added products and the development of competitive products would increase the rate of utilization for small-diameter logs.

The need for the use of small- diameter logs as structural materials has also become an issue in many countries other than Korea, and much related research has been performed to date. For example, in the United States, bending tests and strength performance evaluations based on vibration methods have been implemented to enable the use of small-diameter logs from Douglas-fir, Ponderosa pine, and Western hemlock (Green et al. 2005, 2008; Langum et al. 2009). In Japan, Ishiguri et al. (2006) investigated the physical characteristics and mechanical characteristics of small-diameter logs from Japanese cypress for effective utilization in the civil engineering sector. In Korea, Lee and Kim (1990) studied the sawing and utilization of small-diameter logs. Cha (1996) evaluated whether the bending strength of lamina obtained from small-diameter logs is related to stress wave speed and modulus of elasticity (MOE). Park and Hong (2003) evaluated the bending strength of small-diameter logs using nondestructive and bending tests.

Because timber obtained from small-diameter logs generally has small cross-section dimensions and low strength, its use as structural material is not straightforward. As a result, research focused on laminated beams based and on laminated adhesion of small cross-section timber has been attempted. For example, Hirashima et al. (1988), using

cedar square timber, and Yoshida et al. (2005), using Japanese larch square timber, developed laminated beams and experimentally verified the bending performance. These beams have been limited to vertically laminated adhesion of square timber obtained from small-diameter logs.

This research is conducted with the objective of developing a laminating process for effective utilization of small-diameter logs that include juvenile wood and confirming the possibility of their use as structural materials. Laminated beams and columns are developed from square timber obtained from small-diameter logs. These members are manufactured by vertical and horizontal laminations for getting large dimensions as construction members. These members not only used small-diameter logs but also large-diameter logs for reinforcement of strength and rigidity performance. This research focuses on the bending and compression characteristics obtained by the mechanical tests.

Materials and Methods

Specimen preparation

To prepare specimens from laminated members, square timber and lamina were supplied from the following logs: (1) Japanese larch (*Larix kaemperi* Carr.) small-diameter logs (JL-S), (2) Japanese larch and Douglas-fir (*Pseudotsuga menziesi* Taxifolia) large-diameter logs (JL-L, DF-L), and (3) Japanese larch and Douglas-fir lamina. The Japanese larch and Douglas-fir were grown in Gapyeong-gun, Gyeonggi-do, Korea. The manufacturing process for laminated member specimens was conducted at the Kyung Min Industrial Co. Ltd., Incheon, Korea.

The JL-S used logs aged approximately 20 years with diameters of 120 to 139 mm. The logs were sawn into lumber and then dried and finished to obtain square timber samples with a final cross section of 80 by 80 mm. The yield rate was 42 to 57 percent. Because this square timber was with pith, the vast majority of the material was dominated by juvenile wood. The JL-L and DF-L used logs aged approximately 40 years old with diameters of 300 mm or more. Using the same process as that used for the JL-S, square timber samples were prepared with a cross section of 80 by 80 mm. Because this square timber was without pith, the ratio of the juvenile wood was low. Finally, for the Japanese larch and Douglas-fir lamina, we used lamina specified according to the mechanical grade E14 in KS F 3021 (i.e., bending Young's modulus MOE of 14 to 16 GPa; Korean Standards Association 2010). It should be noted that adjustment was made to values targeting a moisture content of 12 percent.

In preparing the laminated member specimens, excess square timber was manufactured from the JL-S, JL-L, and DF-L. These additional samples were used for investigating the mechanical characteristics in bending and axial compression. It should be noted that finger joints were not used in these additional samples. The results are given in Table 1. As evident from the table, the strength performance without compression strength and yield stress of JL-S was low compared with the others.

Laminated beam specimens

The laminated beam specimens were prepared using the above-mentioned square timber and lamina. Eight types (A, B_{JL}, B_{DF}, C_{JL}, C_{DF}, D_{JL}, D_{DF}, E) of specimens were

Table 1.—Strength characteristics of square timber and lamina.

Test	Square timber (80 × 80 mm in cross section)[a]	Density (g/cm³)	Moisture content (%)	Young's modulus (GPa)	Strength (MPa)	Yield stress (MPa)
Bending	JL-S	0.478	12.5	9.5	46.8	—
	JL-L	0.465	13.4	19.0	54.3	—
	DF-L	0.495	11.3	25.0	68.0	—
	Lamina	—	—	14[b]	54[b]	—
Axial compression	JL-S	0.478	12.5	11.1	37.7	28.0
	JL-L	0.465	13.4	15.7	35.4	19.4
	DF-L	0.495	11.3	24.9	41.1	27.2
	Lamina	—	—	14[b]	32[b]	—

[a] JL = Japanese larch; DF = Douglas-fir; S = small-diameter log; L = large-diameter log.
[b] Mechanical grade E14 in KS F 3021 (Korean Standards Association 2010).

provided as shown in Figure 2 and Table 2. Type A is a four-layer laminated beam using eight pieces of square timber manufactured from JL-S. Type B used square timber manufactured from JL-L or DF-L substituted for the outer layer of Type A (i.e., B_{JL}, B_{DF}). Type C is a laminated beam that uses JL-L or DF-L lamina with a thickness of 35 mm for the outermost layer of Type B (i.e., C_{JL}, C_{DF}). Type D is a laminated beam consisting of the two outermost layers each of JL-L or DF-L lamina with a thickness of 35 mm using four pieces of square timber manufactured from JL-S (i.e., D_{JL}, D_{DF}). In addition, for comparison with the strength performance of general glulam, 12-layer glulam (i.e., Type E) was manufactured from Japanese larch laminae of 33.75 mm thickness. Three specimens of each type were manufactured.

Laminated column specimens

For the laminated column specimens, eight types (F, G_{JL}, G_{DF}, H, J_{JL}, J_{DF}, K_{JL}, K_{DF}) were provided as shown in Figure 2 and Table 3. Type F used four pieces of square timber manufactured from a JL-S and bonded into two layers. Type G used square timber manufactured from JL-L or DF-L substituted for two pieces of square timber positioned in Type F as diagonals (i.e., G_{JL}, G_{DF}). Type H used eight pieces of square timber manufactured from a JL-S and bonded so that the core is hollow. Type J used square timber manufactured from JL-L or DF-L substituted for four-cornered square timber in Type H (i.e., J_{JL}, J_{DF}). Type K is a laminated column with the outer layer of Type F morphologically reinforced with JL-L or DF-L lamina 35 mm thick (i.e., K_{JL}, K_{DF}). No finger joints were used for the square timber and lamina used in all types of laminated column specimens. Three specimens of each type were manufactured.

Adhesion

To ensure the long axis direction length, the square timber and lamina in the laminated beam specimens used vertical finger joints. The finger joint shape consisted of a finger length of 20 mm, a pitch of 6 mm, a tip width of 1 mm, and a slope angle of 7.125°. A polyvinyl acetate (Deernol DF-2000, Oshika Co. Ltd., Tokyo, Japan) was used for the
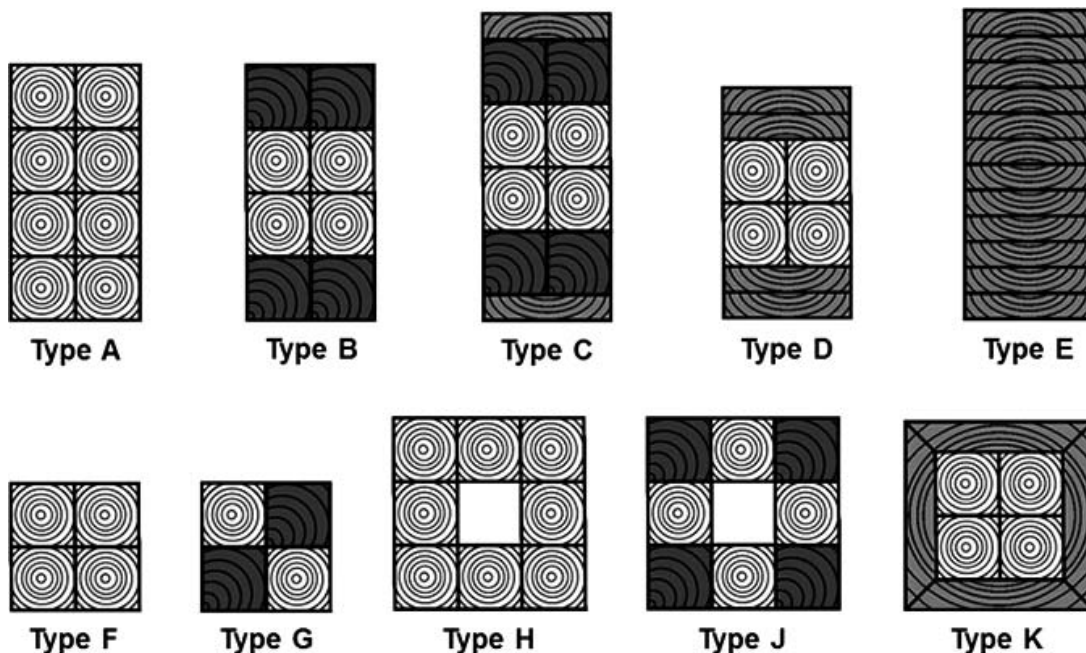

Figure 2.—Composition of laminated beam and column specimen. Details are shown in Tables 2 and 3.

HA ET AL.

Table 2.—Details of laminated beam specimens.[a]

| Type | Cross section (mm) | Square timber (80 × 80 mm) | | Lamina (160 × 35 mm) |
		Inner layer	Outer layer	Outermost layer
A	160 × 320	JL-S[b]	JL-S[b]	—
B$_{JL}$	160 × 320	JL-S[b]	JL-L[c]	—
B$_{DF}$			DF-L[c]	
C$_{JL}$	160 × 390	JL-S[b]	JL-L[c]	JL-L
C$_{DF}$			DF-L[c]	DF-L
D$_{JL}$	160 × 300	JL-S[b]	—	JL-L
D$_{DF}$				DF-L
E	150 × 405	—	—	JL-L[d]

[a] $n = 3$ specimens of each type. JL = Japanese larch; DF = Douglas-fir; S = small-diameter log; L = large-diameter log.
[b] Bright part of square timber in Figure 2.
[c] Dark part of square timber in Figure 2.
[d] 150 by 33.75 mm.

finger adhesive. The adhesive information, spread, pressure, assembly time, and ratio of base resin to hardener are shown in Table 4.

The laminated beam and laminated column specimens were prepared in the order shown below. To glue the square timber and lamina, we first performed the adhesion within the same layer (i.e., edge gluing) using aqueous polymer isocyanate (Shikajirusi PI Bond TP-111, Oshika Co. Ltd.). Afterward, the adhesion between the layers (i.e., laminated adhesion) was performed using phenol-resorcinol-formal-dehyde (Deernol D-40, Oshika Co. Ltd.).

Bending test

For the bending test, this research was performed by the test method shown in Figure 3 in conformance with ASTM D198 (ASTM International 2009). This test was conducted using a bending tester (Dongah Testing Machine Co., Seoul, Korea; capacity, 50 ton force [tonf]) for full-scale materials to implement a trisection point, third-point bending test. Span ℓ was set to 3,600 mm, and the load point was set to 1,200 mm (i.e., $= \ell/3$). The loading speed was set to 10 mm/min. Two linear variable differential transformers LVDTs (DEX-01-V, Mutoh Engineering Inc., Tokyo, Japan) were attached to the central area and both side surfaces of the specimen to measure the central deflection δ.

This bending test was used to find the bending rigidity (EI), bending Young's modulus (MOE), and bending strength (modulus of rupture [MOR]) based on the following equations:

$$EI = \frac{23l^3}{108bd^3} \cdot \frac{\Delta P}{\Delta \delta} \cdot \frac{bd^3}{12} \quad (1)$$

$$MOE = \frac{23l^3}{108bd^3} \cdot \frac{\Delta P}{\Delta \delta} \quad (2)$$

$$MOR = \frac{P_{b\max}l}{bd^2} \quad (3)$$

where b is the beam width, d is the beam depth, $\Delta P/\Delta \delta$ is defined as a relationship between the slope of the elastic region for the load P–deflection δ, and $P_{b\max}$ is the maximum bending load.

Axial compression test

The axial compression test was performed in conformance with ASTM D198 (ASTM International 2009) based on the setup shown in Figure 4. This test was conducted using a compression tester (Samduk Engineering Co., Seongnam, Korea; capacity, 200 tonf). The loading speed was set to 10 mm/min. The axial compression load P was applied with the top part of the specimen fixed in place. The long axial direction length ℓ of the specimen was 2,600 mm. Two sliding resistance type displacement transducers (TCLA-100B, Showa Measuring Instruments Co. Ltd., Tokyo, Japan) were mounted on both sides of the specimen and measured the specimen axial compression displacement δ. It should be noted that when testing column specimens, determining the buckling characteristics was important.

Table 3.—Details of laminated column specimens.[a]

Type	Cross section (mm)	Square timber (80 × 80 mm)	Lamina (230 × 35 mm)
F	160 × 160	JL-S	—
G$_{JL}$	160 × 160	JL-S[b] + JL-L[c]	—
G$_{DF}$		JL-S[b] + DF-L[c]	
H	240 × 240	JL-S	—
J$_{JL}$	240 × 240	JL-S[b] + JL-L[c]	—
J$_{DF}$		JL-S[b] + DF-L[c]	
K$_{JL}$	230 × 230	JL-S	JL-L
K$_{DF}$		JL-S	DF-L

[a] $n = 3$ specimens of each type. JL = Japanese larch; DF = Douglas-fir; S = small-diameter log; L = large-diameter log.
[b] Bright part of square timber in Figure 2.
[c] Dark part of square timber in Figure 2.

Table 4.—Adhesives used and adhesive conditions.

Adhesive[a]	Viscosity (Pa·s)	pH	Solids content (%)	Spread (g/m²)	Pressure (kgf/cm²)	Assembly time	Ratio of base resin to hardener
Polyvinyl acetate (PVAc)	0.63	10.8	60.4	400–500	19.6–90.8	1 s	100:0
Aqueous polymers isocyanate (API)	10.0	6.4	60.0	230–270	7.8–9.8	4 h	100:15
Phenol-resorcinol-formaldehyde (PRF)	0.36	8.5	58.5	250–350	9.8–10.8	22 h	100:15

[a] PVAc was used in finger-jointing of square timber and lamina. API was used in primary adhesion within same layer (i.e., edge gluing). PRF was used in secondary adhesion between layers (i.e., laminated adhesion).

Therefore, an antibuckling support was not provided as shown in Figure 4.

The axial compression test was used to determine the compression Young's modulus (E_c), the yield stress (σ_{cy}), and the compression strength (σ_{cmax}). E_c was calculated based on the following equation:

$$E_c = \frac{l}{A} \cdot \frac{\Delta P}{\Delta \delta} \qquad (4)$$

where A is the cross-section area, and $\Delta P/\Delta \delta$ is defined as the relationship between the slope of the elastic region in the load P–displacement δ.

The parameters σ_{cy} and σ_{cmax} were determined based on the following equations:

$$\sigma_{cy} = \frac{P_{cy}}{A} \qquad (5)$$

$$\sigma_{cmax} = \frac{P_{cmax}}{A} \qquad (6)$$

where P_{cy} is the yield load (maximum load of the elastic region in the P–δ), and P_{cmax} is the maximum axial compression load.

Results and Discussion
Bending load–deflection relationship

In the bending test for the laminated beam specimens, the typical load P–deflection δ relationship for each specimen type is shown in Figure 5. Note that once the strength characteristic values were determined, the P–δ data for Type A were lost owing to an accident. As a result, the curve for A is not shown in Figure 5.

Every type showed a straight-line P–δ relationship from the initial load to failure. For Type E, the cross section was large, and the rigidity and maximum bending load were the largest of all the types. Type C had cross-section dimensions close to Type E, and the Type C_{DF} rigidity was close to Type E. Nevertheless, a failure occurred when the deflection was around 30 mm, falling below the Type E maximum deflection of approximately 40 mm. The rigidity and maximum bending load for Types B and D were smaller when compared with the above-mentioned Types C and E.
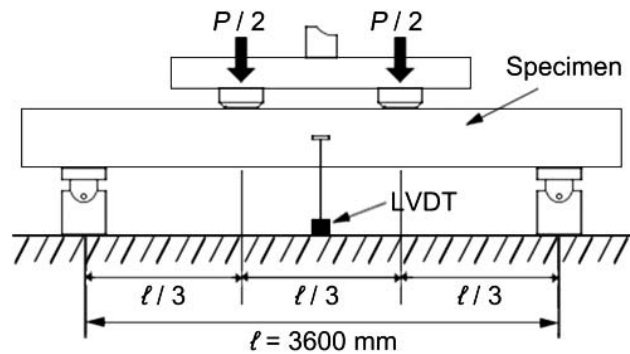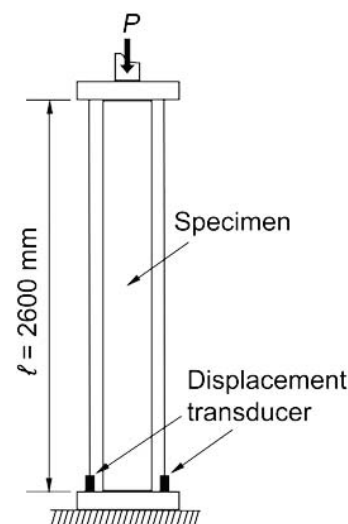

Figure 3.—Bending test method.

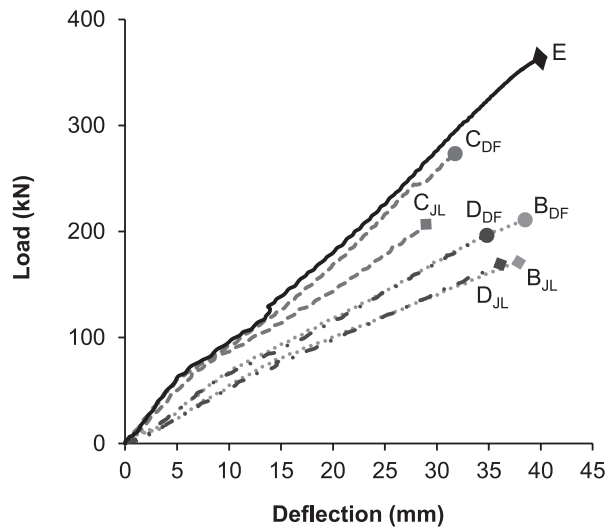Figure 4.—Axial compression test method.

Figure 5.—Examples of relationship between bending load and deflection.

This is owing to the smaller cross-section dimensions. In Figure 5, the P–δ relationships of Types B and D were similar curves, suggesting that they have an equivalent degree of resistance performance.

When examining differences in the species used for the outer layers of these specimens, in other words the square timber or lamina species, specimens manufactured using Douglas-fir (B_{DF}, C_{DF}, D_{DF}) showed a higher rigidity than the specimens using Japanese larch (B_{JL}, C_{JL}, D_{JL}). As

given in Table 1, the reason appears to be that DF-L has a higher bending Young's modulus than JL-L.

Bending failure mode

The failure mode observed in the laminated beam specimens at the time of the bending test is shown in Figure 6. At maximum bending load, cracks appeared in the outermost layer, particularly near knots and other defect points. Simultaneously with the appearance of cracks, the resistance of the specimens decreased drastically. These cracks progressed toward a knot in the inner layer, as shown in Figure 6a. In addition, as shown in Figure 6b, cracks propagated in the adhesion layer in a section of the specimen causing delamination of the adhesion layer. These failure modes were shared by all types and species.

Bending rigidity and bending Young's modulus

Using Figure 5, the following bending characteristics were determined as shown in Figure 7: bending rigidity (EI), bending Young's modulus (MOE), maximum bending load ($P_{b\max}$), bending strength (MOR), and maximum deflection ($\delta_{b\max}$). The figure shows the average value for each specimen type and notes their standard deviation as reference data because the number of specimens is small.

Figure 7a shows EI and MOE for each specimen type. For Type A, $EI = 3{,}948$ kNm^2 and MOE $= 9.0$ GPa were lower compared with the other types. This is due to a high ratio of juvenile wood in the square timber for this type, resulting in low strength performance, as given in Table 1. In contrast, for Types B, C, and D, MOE values are as follows: B_{JL}, 11.2
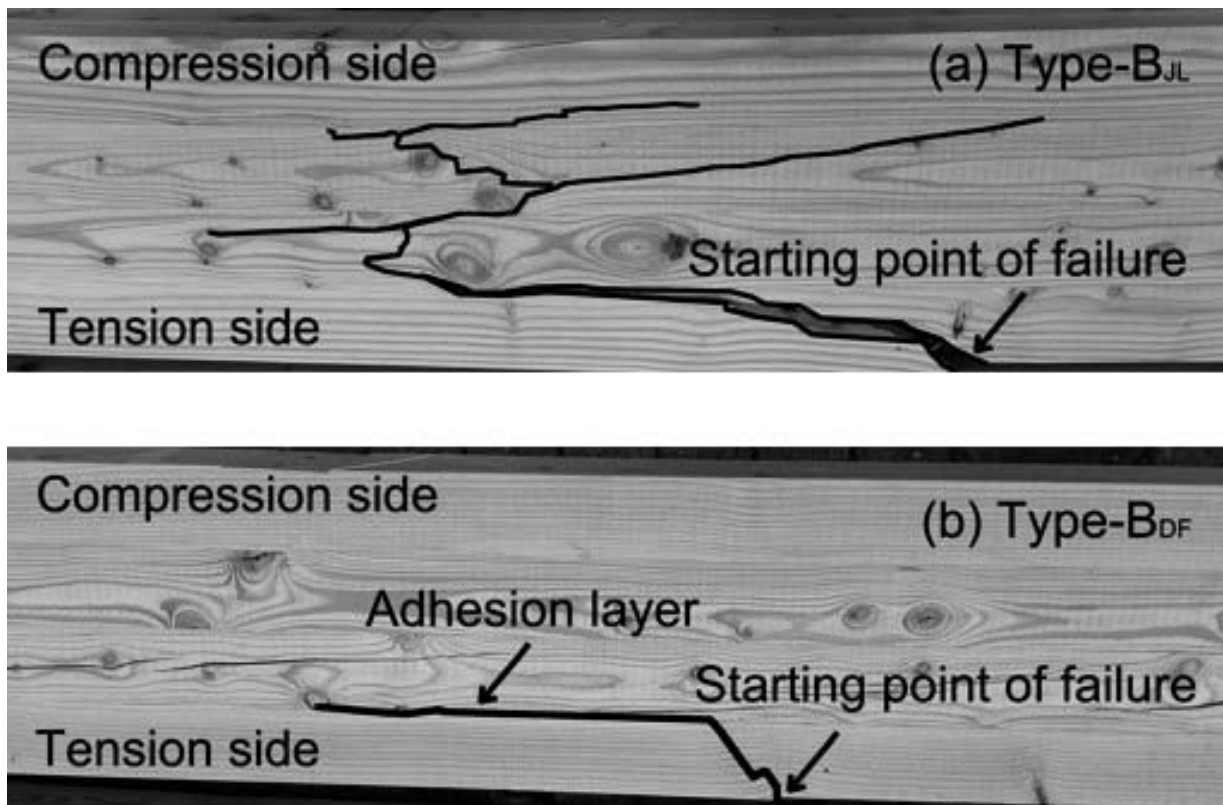

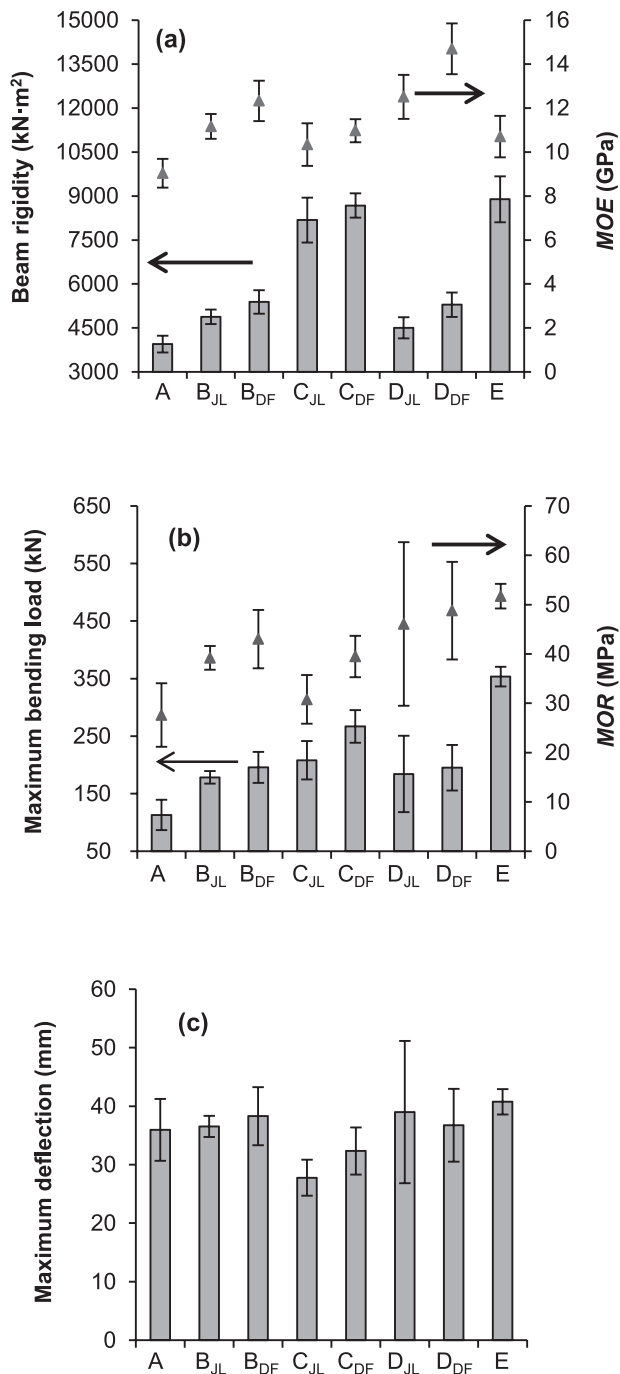Figure 6.—Bending failure mode for laminated beams.

Figure 7.—Comparisons of laminated beam bending characteristic values by type, for (a) bending Young's modulus and bending rigidity, (b) bending strength and maximum bending load, and (c) maximum deflection.

GPa; B_{DF}, 12.3 GPa; C_{JL}, 10.3 GPa; C_{DF}, 11.0 GPa; D_{JL}, 12.5 GPa; D_{DF}, 14.7 GPa for all species. Additionally, MOE values for Types B, C, and D were not inferior compared with Type E (10.7 GPa). Hence, in an evaluation based on MOE, it is suggested that these three types have the potential for use as structural beams.

According to the graph, for Types C and E, MOE showed smaller values than for Types B and D, while *EI*

increased sharply. This is because Types C and E appear to have a size effect owing to their large cross section (i.e., beam depth). Furthermore, since the beam depth *d* compared with the span ℓ is large (i.e., $\ell/d = 8.89$ to 9.23), MOE appears to be evaluated as smaller because the shear deformation of the specimens arising during the test became larger.

When an analysis of variance was performed on the above MOE results, a significant difference was found at 5 percent. Moreover, when a multiple comparison procedure (Tukey method) was performed, a significant difference (5% level) was found only between Types A and D_{DF}.

Maximum bending load and bending strength

Figure 7b shows the maximum bending load ($P_{b\max}$) and bending strength (MOR) for each specimen type. According to this, MOR for Type E was the largest at 51.7 MPa, while Type D showed a value virtually equivalent to this for both species (D_{JL}, 46.1 MPa; D_{DF}, 48.8 MPa). On the other hand, for Type A, MOR was lower at 27.6 MPa, while for Types B and C with reinforcement applied, an improvement in MOR was observed (B_{JL}, 39.2 MPa; B_{DF}, 43.0 MPa; C_{JL}, 30.8 MPa; C_{DF}, 39.5 MPa). Note that for Type A, MOR declined sharply even when compared with the JL-S of 46.8 MPa (Table 1). The reason for this decline appears to be that the finger joints are included in the square timber prepared for the laminated beam specimens. While a significant difference was found in the analysis of variance of the above MOR results, when the multiple comparison procedure (Tukey method) was used, no difference due to type was found.

For the $P_{b\max}$, a size effect was found owing to the size of the beam depth. In addition, while also related to the maximum deflection discussed in the next section, the Type D failure point showed quite a large scatter, and it appears that the effect of two-layer lamina quality composing the outermost layer is significant.

Maximum deflection

Figure 7c shows the maximum deflection $\delta_{b\max}$. With the exception of Type C_{JL}, $\delta_{b\max}$ was found to be 30 to 40 mm for all types. A comparison of Types B and C showed that $\delta_{b\max}$ in Type C decreased. Therefore, it appears that the addition of a single layer of lamina to the outermost layer has the effect of restricting deformation.

Compression load–displacement relationship

In the axial compression test for the laminated column specimens, the typical compression load *P*–displacement δ relationship for each specimen type is shown in Figure 8. Note that once the strength characteristic values were determined, the data for Types F and H were lost owing to an accident. As a result, the curves for Types F and H are not shown in Figure 8.

Unlike the bending test case, all types showed a nonlinear *P*–δ relationship. After the yield point, maximum axial compression load was attained followed by a decline in resistance. Types J and K had a large cross-section area leading to significant rigidity and large maximum axial compression load.
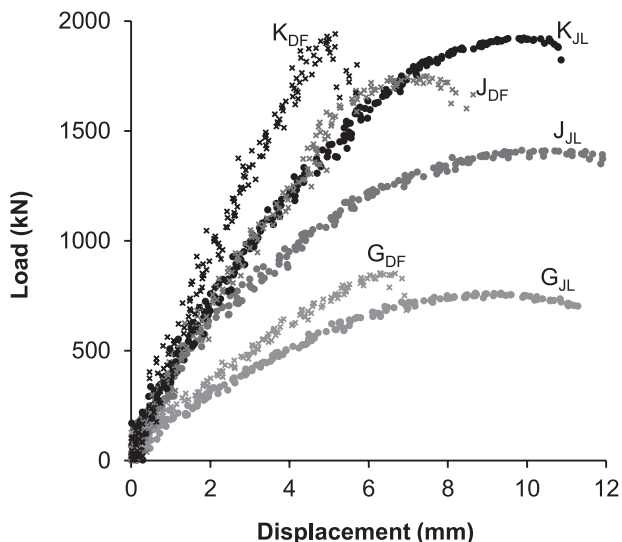
Figure 8.—Examples of relationship between compression load and displacement.

Compression failure mode

The compression failure mode is shown in Figure 9. As shown in Figure 9a, buckling appeared near the column central areas in Types F and G. This was due to the large slenderness ratio based on a small cross-section area and because the axial compression displacement for both types was large compared with the other types. As shown in Figures 9b and 9c, the failure mode of Types H and J resulted in buckling owing to the multiple causes of grain angle with the adhesion layer (Fig. 9b) and grain angle with knots (Fig. 9c). In particular, delamination of the adhesion layer was dominant. These types of cross-section shapes have a hollow space, which became an apparent weak point. Type K failure mode was due to the end bearing, as shown in Figure 9d. This type of failure mode occurred because Type K has a small slenderness ratio and a small axial compression displacement compared with other types.

Compression Young's modulus

The compression Young's modulus E_c is shown in Figure 10. The figure indicates a trend that is dependent on the specimen type. Types F and H using square timber obtained from JL-S showed the smallest E_c (F, 9.8 GPa; H, 8.1 GPa). These values were less than the values given in Table 1 of 11.1 GPa owing to lamination. Types G and J utilizing square timber obtained from JL-L and DF-L showed an increase in E_c. Moreover, when Douglas-fir was used, E_c was large (G_{JL}, 10.4 GPa; G_{DF}, 13.6 GPa; J_{JL}, 11.5 GPa; J_{DF}, 16.2 GPa). For Type K with a lamina of 35 mm thickness obtained from large-diameter logs, E_c greatly increased (K_{JL}, 14.5 GPa; K_{DF}, 20.7 GPa). While a significant difference was found in the analysis of variance for the above results of E_c, when the multiple comparison procedure (Tukey method) was used no difference was found.

Yield stress and compression strength

Figure 11 shows the yield stress σ_{cy} and compression strength σ_{cmax}. The average value of the respective types related to σ_{cy} was 17.4 to 24.0 MPa, and σ_{cmax} was 27.7 to
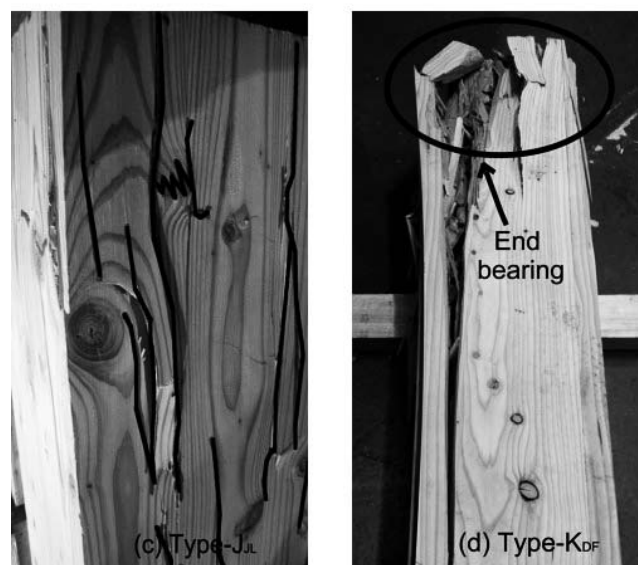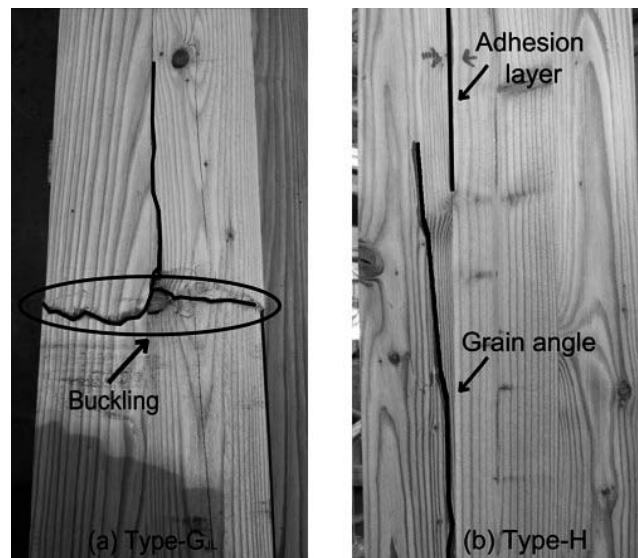

Figure 9.—Compression failure mode for laminated beams.

35.4 MPa. When the analysis of variance and multiple comparison procedures (Tukey method) were performed, no significant difference was seen between the eight types. The relationship was similar to compression Young's modulus ratio trend shown in Figure 10.

Critical stress

The critical stresses σ_{cr} of the laminated column were determined based on Euler's and Johnson's equations.

The Euler buckling equation (Mott 2007) excludes the buckling load P_{cr} from the cross-section area A and can be determined based on the following equation:

$$\sigma_{cr} = \frac{P_{cr}}{A} = \frac{\pi^2 E}{(K\ell/k_z)^2} \qquad (7)$$

where $K\ell/k_z$ is the slenderness ratio of the column, and E is Young's modulus. As the test conditions rotate around both ends, $K = 1.0$.
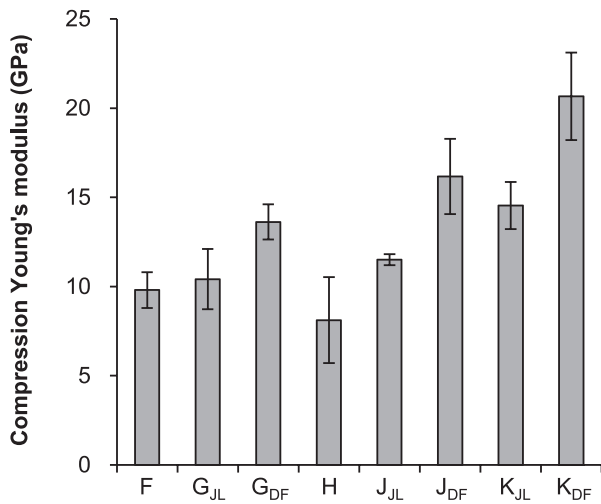
Figure 10.—Compression Young's modulus of laminated columns.

Figure 11.—Yield stress, compression strength, and critical stress of laminated columns.

By setting the materials yield stress σ_0, the Johnson buckling equation (Mott 2007) can be expressed as follows:

$$\sigma_{cr} = \sigma_0 \left\{ 1 - \frac{\sigma_0}{4\pi^2 E} \left(\frac{K\ell}{k_z} \right)^2 \right\} \qquad (8)$$

In addition, E and σ_0 were the axial compression characteristic values of square timber and lamina given in Table 1. For Types G, J, and K, E and σ_0 were the smallest values of the respective square timber and lamina.

The critical stress based on Euler's equation is shown in Figure 11 as triangles. The calculated value was 34.5 to 86.3 MPa, and for every type greatly exceeded the compression strength. In particular, as the column cross section grows larger, it shows a tendency to deviate significantly. While it is known that if the yield stress in a long column has a larger slenderness ratio, it generally matches Euler's equation. Therefore, if the slenderness ratio becomes smaller, Euler's equation cannot be applied. The results from Figure 11 confirmed this limitation. Meanwhile, the calculated value based on Johnson's equation was 16.7 to 25.7 MPa (shown as solid circles) and was positioned near the yield stress of each type. In the estimates for critical stress that are related to the eight types of laminated columns produced in this research, it is suggested that the application of Johnson's equation is desirable.

Conclusions

There are a large number of small-diameter logs, and the effective utilization of these timber resources is desirable. In particular, utilization as structural materials would result in relatively high-value-added and has therefore attracted much interest. Because small-diameter logs are composed of significant juvenile wood, they do not have sufficient strength performance and are unsuitable as structural materials. As a result, in this research, square timber or lamina from large-diameter logs was added to square timber obtained from small-diameter logs to develop laminated beams and laminated columns treated with mechanical reinforcement. These members were manufactured by the vertical and horizontal laminations from square timber for
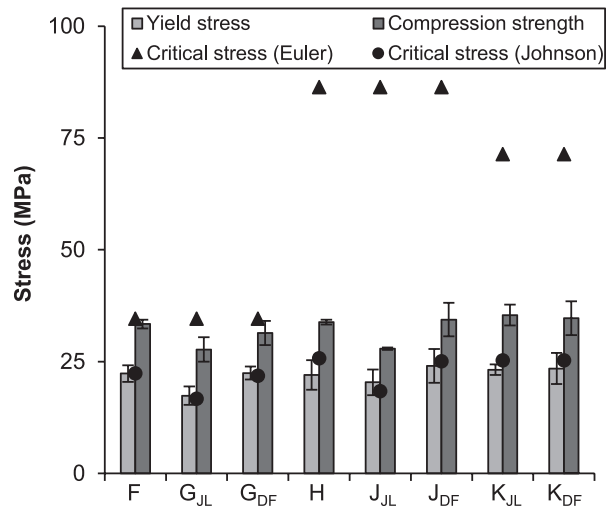
getting large dimensions. The strength performance was then experimentally verified.

A bending test on the laminated beam specimens was performed to find MOE and MOR. For the specimens using only square timber obtained from small-diameter logs, MOE was 9.0 GPa, which was less than the 10.7 GPa of the glulam based on the conventional lamina layers. By contrast, specimens reinforced with square timber or lamina from large-diameter logs had an MOE of 10.3 to 14.7 GPa, indicating that these specimens had values either the same or higher than the glulam. Specimens using only square timber obtained from small-diameter logs had an MOR of 27.6 MPa, which was relatively low. By contrast, specimens reinforced with square timber or lamina from large-diameter logs had an MOR of 30.8 to 48.8 MPa, thereby confirming an improvement in the MOR.

The compression Young's modulus values for two specimen types using only square timber obtained from small-diameter logs were 9.8 and 8.1 GPa, as determined by the laminated column axial compression test. In contrast, the specimens reinforced with square timber or lamina from large-diameter logs had a compression Young's modulus ranging from 10.4 to 20.7 GPa, thereby confirming a sufficient reinforcement effect. Additionally, regarding the yield stress and compression strength, it was a similar reinforcement effect. When Johnson's equation was used to calculate the critical stress, it was calculated in the range of 16.7 to 25.7 MPa. This value was close to the yield stress for all types. Therefore, it was shown that the critical stress for the laminated column produced in this research could be predicted using Johnson's equation.

While the strength and rigidity performance of the laminated beam and laminated column consisting only of square timber obtained from small-diameter logs was not very high, it was able to confirm that implementation of reinforcement using square timber or lamina from large-diameter logs can improve its strength performance. In addition, based on the strength performance of the reinforced specimens, it is possible to use the small-diameter logs as structural materials.

Acknowledgments

Literature Cited

ASTM International. 2009. Standard test methods of static tests of lumber in structural sizes. ASTM D198. ASTM International, West Conshohocken, Pennsylvania.

Cha, J. K. 1996. Study on stress waves for development of glulam from domestic small diameter log (II)—Static bending properties of glulam member. *J. Korean Wood Sci. Technol*. 24(4):7–14.

Green, D. W., T. M. Gorman, J. W. Evans, J. F. Murphy, and C. A. Hatfield. 2008. Grading and properties of small-diameter Douglas-fir and ponderosa pine tapered logs. *Forest Prod. J*. 58(11):33–41.

Green, D. W., E. C. Lowell, and R. Hernandez. 2005. Structural lumber from dense stands of small-diameter Douglas-fir trees. *Forest Prod. J*. 55(7/8):42–50.

Hirashima, Y., S. Oshiumi, A. Inoue, Y. Ono, and K. Komatsu. 1988. Bending strength of glued-timber beams built-up from square timbers. *Mokuzai Kogyo* 43(2):14–19. (In Japanese.)

Ishiguri, F., J. Eisawa, Y. Saito, K. Iizuka, S. Yokota, and N. Yoshizawa. 2006. Comparison of wood properties of Hinoki (*Chamaecyparis obsta*) small diameter logs collected from different tree ages and heights. *Mokuzai Gakkaishi*. 52(6):383–388. (In Japanese.)

Korea Forest Service. 2015. Statistical Yearbook of Forestry. Korea Forest Service, Daejeon. pp. 286, 332–333. (In Korean.)

Korea Forest Service and Korea Forestry Promotion Institute. 2013. Assessment of the Korea's Forest Resources. Korea Forestry Promotion Institute, Seoul. pp. 94, 254. (In Korean.)

Korean Standards Association. 2010. Structural glued laminated timber. KS F 3021. Korean Standards Association, Seoul. (In Korean.)

Langum, C. E., V. Yadama, and E. C. Lowell. 2009. Physical and mechanical properties of young-growth Douglas-fir and western hemlock from western Washington. *Forest Prod. J*. 59(11/12):37–47.

Lee, C. T. and S. C. Kim. 1990. A study on sawing and utilization structure of lumber from small-diameter logs of *Larix leptolepis*. *J. Korean Wood Sci. Technol*. 18(3):53–68. (In Korean.)

Mott. R. L. 2007. Applied Strength of Materials. 5th ed. CRC Press, Boca Raton, Florida. 611 pp.

Park, J. C. and S. I. Hong. 2003. Bending strength assessment of Larix logs by nondestructive evaluation techniques. *J. Korean Forest Soc*. 22(2):60–68. (In Korean.)

Yoshida, T., Y. Itoh, and T. Hashizume. 2005. Fabrication of a vertically laminated beam composed of two Japanese larch beams and its bending strength. *Mokuzai Kogyo* 60(2):65–69. (In Japanese.)